OTFS Achievable Ranging Performance in LEO Urban Areas

Guillem Foreman-Campins
Tampere University, Finland
Universitat Autònoma de Barcelona, Spain
guillem.foremancampins@tuni.fi

José A. López-Salcedo
Universitat Autònoma de Barcelona
Bellaterra, Spain
jose.salcedo@uab.cat

Elena Simona Lohan
Tampere University
Tampere, Finland
simona.lohan@tuni.fi

***Abstract*—During the past decades, seamless navigation has become crucial for numerous Position-Navigation-Timing (PNT)-based applications, with Global Navigation Satellite Systems (GNSS) serving as the primary provider for PNT solutions. However, GNSS faces limitations and severe threats which are limiting to the increasing needs in positioning applications. The use of Low-Earth-Orbit (LEO) satellites for positioning is projected to be a strong alternative to standard GNSS due to its potential improvements in key metrics for positioning. In this regard, the present paper unveils the use of the Orthogonal Time Frequency Space (OTFS) modulation for a standalone LEO-PNT system, and it discusses how OTFS can be tailored to any LEO-PNT scenario to obtain excellent multipath mitigation capabilities. Specifically, these are achieved by using the Doppler characterisation of LEO multipath signals, which combines well with the high Doppler resolution of OTFS. A statistical analysis on the relative delay and Doppler of the reflected signals is conducted during several passes of two real LEO satellites over a receiver in an urban environment, from which OTFS is configured given a requirement on ranging accuracy. Subsequently, the hypothetical use of OTFS for these two real LEO satellites is analysed through simulations on its ranging accuracy, demonstrating its improvements over the standard Binary Phase Shift Keying (BPSK) modulation used in GNSS.**

***Index Terms*—LEO-PNT, OTFS, delay-Doppler processing**

I. Introduction

In recent years, positioning services have seen a substantial increase in the demands for high accuracy and reduced complexity, driving the need for enhanced and revamped solutions that overcome the limitations of GNSS [1], [2]. One such solution is the employment of alternative systems to complement the GNSS constellations, and particularly the use of Low Earth Orbit (LEO) satellites, commonly referred as the LEO Position-Navigation Timing (LEO-PNT) solution, which have been shown to provide prominent advantages for positioning services [3]–[5]. Inherently, LEO satellites yield signals with higher received power than GNSS, which give higher Carrier-to-Noise ratios (C/N_0) and stronger robustness to intentional and unintentional interferences. Furthermore, LEO satellites are subject to faster time-varying multipath, along with improved Geometric Dilution of Precision (GDOP). It is for this reason that, when used complementarily to GNSS, LEO-PNT is expected to add the layer of integrity, security and sovereignty that many governmental bodies and industrial partners are seeking for next-generation satellite-based positioning systems [6].

All these advantages have triggered the study of future dedicated LEO-PNT constellations within both public and private institutions. Among all the features to be carefully addressed, the signal design stands out as particularly important due to its critical role in ensuring the system's performance and reliability, while keeping low complexity to encourage adoption in small devices with constraints on power consumption and computational load (e.g. devices for Internet of Things applications). This latter feature is actually one of the GNSS Achilles' heel, and it is intended to be circumvented in future LEO-PNT signal designs through the use of more efficient signaling schemes. To this end, several signal modulations are currently under study for their use in LEO-PNT such as Chirp Spread Spectrum (CSS) [7], Orthogonal Frequency Division Multiplexing (OFDM), due to its synergies with signals envisaged to be used in 5G non-terrestrial networks (NTN) [8], and GNSS-like signals better tailored to LEO scenarios, and thus using lower chipping rates and shorter codes than in conventional GNSS [9].

In this context, the present work intends to unveil the interest of the Orthogonal Time Frequency Space (OTFS) modulation, a variant of OFDM first proposed in [10] for communications in highly time-variant multipath channels [11]. OTFS is engineered by adding an extra layer to OFDM by means of a Symplectic Fourier transform (SFFT), which translates from the time-frequency domain of OFDM into the so-called delay-Doppler (DD) domain, or otherwise by using the Zak transform representation of time-domain signals [12]. Such a design keeps the Bit-Error-Rate (BER) low in highly dynamic scenarios, since each symbol in the DD domain has an improved resolution directly related to the channel, which makes them more time-invariant and thus robust to Inter-Carrier Interference (ICI) [12].

Notably, a myriad of disciplines are considering the use of OTFS, from future 5G/6G wireless networks [13], next-generation radar systems [14]–[17], devices for Internet of Things (IoT) [18]–[20], and most recently, Integrated Sensing and Communications (ISAC) [21]–[23]. The interest is not only due to the OTFS robust performance in high-mobility scenarios, but also to its direct interaction with the delay-

This work was supported by the INCUBATE project funded by the Technology Industries of Finland Centennial Foundation and the Jane and Aatos Erko Foundation. This work was also supported by the LEDSOL project, funded by the EU Horizon 2020 Research and Innovation Program (grant 963530), by the Research Council of Finland (grant 352364) and partly supported by the Spanish Agency of Research (projects PDC2023-145858-I00 and PID2023-152820OB-I00).

979-8-3503-5685-4/24/$31.00 ©2024 IEEE

Doppler (DD) domain of the channel. Such interaction mirrors the underlying physical geometries of the environment, allowing different reflected paths to be separated. In the communication arena, this is clearly used to mitigate ICI, but in the positioning arena, this feature can also be used for sensing the environment, thus bringing an interesting added value in the aforementioned applications dealing with ISAC.

While most of the existing contributions on OTFS focus on terrestrial applications, little attention has been drawn so far to the possibility of using OTFS for satellite-based positioning. In this context, the present paper extends the results in [24], by analysing a real-case scenario for LEO-based positioning in urban environments. To this end, numerical results are obtained from a Matlab ray-tracing engine for a user terminal located in downtown Hong Kong and receiving signals from a set of Starlink satellites. The ray-tracing results provide valuable insights on the delay-Doppler spread that can be expected in this type of scenarios. These insights serve as a guideline for designing the delay-Doppler grid of prospective OTFS schemes for LEO-PNT, and to assess their achievable ranging performance.

II. OTFS Fundamental Concepts for LEO-PNT

A. OTFS signal model

The properties of the OTFS signal are given by its ability to convert a doubly-dispersive time-domain channel into a sparse and separable set of taps in the delay-Doppler (DD) domain. To do so, the available two-sided bandwidth B is divided into M subcarriers with separation $\Delta f = B/M$. Similarly, the available time for transmitting a so-called OTFS block or frame is divided into N consecutive time slots, each of duration $T = 1/\Delta f$ seconds. Assuming for simplicity that a rectangular pulse shape is used, parameters M and N are then the ones characterizing the discrete-time performance of the OTFS signal.

In the DD domain, a set of MN symbols are stacked into an $M \times N$ matrix $\mathbf{X}_{\mathrm{DD}}$, corresponding to the bins of an $M \times N$ DD grid. The MN DD symbols are then transformed into a set of MN time-frequency (TF) symbols as follows,

$$[\mathbf{X}_{\mathrm{TF}}]_{n,m} = \frac{1}{\sqrt{MN}} \sum_{p=0}^{N-1} \sum_{q=0}^{M-1} [\mathbf{X}_{\mathrm{DD}}]_{q,p}\, e^{j2\pi(\frac{mp}{N} - \frac{nq}{M})} \quad (1)$$

with $\mathbf{X}_{\mathrm{TF}}$ an $M \times N$ time-frequency matrix, and then these symbols are transmitted similarly to a conventional OFDM signal [25]. That is, the baseband equivalent of the resulting discrete-time OTFS transmitted signal $s(k)$ is given by

$$s(k) = \frac{1}{M\sqrt{N}} \sum_{k=0}^{N-1} \sum_{m=0}^{M-1} [\mathbf{X}_{\mathrm{TF}}]_{k,m}\, e^{j2\pi \frac{m}{M} k} \quad (2)$$

for $k = 0, \ldots, MN-1$. Interestingly, the MN signal samples of the OTFS signal can be stacked into the $(MN \times 1)$ vector $\mathbf{s}$ and thus conveniently expressed in matrix form as,

$$\mathbf{s} = \frac{1}{M} \mathrm{vec}(\mathbf{X}_{\mathrm{DD}} \mathbf{F}_N^H). \quad (3)$$

with $\mathbf{F}_N$ the $(N \times N)$ Fourier matrix such that $[\mathbf{F}_N]_{p,q} \doteq \frac{1}{\sqrt{N}} e^{-j2\pi pq/N}$ and thus $\mathbf{F}_N \mathbf{F}_N^H = \mathbf{I}_N$.

B. OTFS Doppler-delay resolution

We consider the following signal model for the received signal in an N_p-path multipath channel,

$$r(k) = \alpha_0 s(k-\tau) e^{j2\pi k\nu} + \sum_{l=1}^{N_p} \alpha_l s(k-\tau-\tau_l') e^{j2\pi k(\nu+\nu_l')} + w(k) \quad (4)$$

where α_l for $l = 0 \ldots, N_p$ denotes the amplitude of each replica, ν and τ the delay and Doppler of the line-of-sight (LoS), while ν' and τ' represent the relative Doppler and delay of the multipath with respect to the LoS, respectively. Finally, $w(k)$ contains the thermal noise.

According to the considerations discussed in Section II-A, the DD domain of the OTFS signal has a delay resolution given by $\Delta\tau = 1/B$ and a Doppler resolution of $\Delta\nu = \frac{B}{MN}$. This shows that the resolution in the Doppler domain depends on both the number of subcarriers M but also on the number of slots N, which corresponds to the number of consecutive OFDM symbols that form an OTFS frame. This concatenation of OFDM symbols is actually what brings OTFS the capability of coping with time-varying multipath channels.

Because of the strong dynamics of the LEO satellite, the relative Doppler of the multipath with respect to the LoS is not negligible, as is instead for MEO satellites. Its value is given by $\nu' = \frac{f_c}{c} \cdot \frac{\partial \Delta d}{\partial t}$, with f_c the carrier frequency and Δd the path distance difference between multipath and LoS. Depending on the distribution of ν' within a given working scenario, the OTFS Doppler resolution $\Delta\nu$ can be properly configured so as to make the reflected paths separable in the DD domain.

C. Adjusting OTFS to accuracy requirements

Following the logic described in the previous subsection, the OTFS design goal considered in this work aims at setting $\Delta\nu$ and $\Delta\tau$ so that they allow the paths of a LEO doubly-spread channel to be separable in the DD domain.

For a certain ν' and τ', the multipath-induced ranging estimation error of OTFS is approximated by,

$$e_{\tau,\mathrm{MP}}(\tau', \nu') \approx e_{\tau,\mathrm{MP}}(\tau', \nu' = 0) \cdot \mathrm{sinc}(2\nu'/\Delta\nu) \quad (5)$$

with $e_{\tau,\mathrm{MP}}(\tau', \nu' = 0)$ the value of the Multipath Error Envelope as portrayed in [24] for a particular τ' and $\nu' = 0$.

Notably, Eq. (5) directly relates the delay error with the OTFS Doppler resolution, thus relating the configuration of parameters *M*, *N* and *B* with the ranging estimation accuracy. These can be related because of the OTFS signal design, with the accuracy improving as the paths stop overlapping in either one of the Doppler and delay dimensions.

From Eq. (5), given some requirement on the delay estimation accuracy and a certain statistical distribution of the values of ν' and τ', the OTFS parameters *M*, *N* and *B* can be designed so that they produce a $\Delta\nu$ that fits said requirement. As an example, the relation between $\Delta\nu$ and the delay accuracy is further shown in Fig. 1 where we take $\tau' = 30$ m, which results in an $e_{\tau,\mathrm{MP}}(\tau', \nu' = 0)$ of -4.68 m [24], and show the different errors produced for various choices of $\Delta\nu$. This goes to show that $\Delta\nu$ can be designed according to a given statistical requirement on $e_{\tau,\mathrm{MP}}$ and given the distributions

of ν' and τ'. Fig. 1 also depicts the difference between the simulated values of $e_{\tau,\mathrm{MP}}$ with the model in Eq. (5).

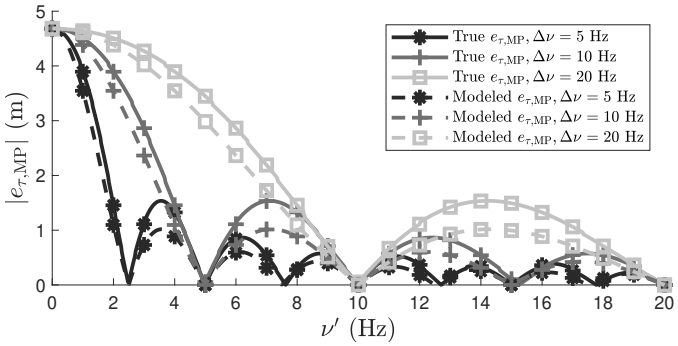

Fig. 1: Representation of $e_{\tau,\mathrm{MP}}$ with respect to ν', for various values of $\Delta\nu$, and taking $\tau' = 30$ m.

In Section III, the exact τ' and ν' distributions in LEO multipath scenarios are obtained, and Section IV follows with the $\Delta\nu$ definition using the developments in this subsection, for the obtained distributions and a delay accuracy requirement.

III. Empirical LEO Delay-Doppler Distribution

A. Scenario definition

The considered received LEO signal is defined by Eq. (4). As mentioned in the previous section, the strong dynamics of the LEO channel yield non-negligible values of ν', which mainly depend on the satellite altitude and the multipath geometry of the receiver. The characterisations of ν' and τ' in LEO scenarios are obtained in this section, for one particular receiver position and taking data from real LEO satellites. Notably, τ' and ν' depend only on the geometry of the system and not on the signal design, and thus we take data about the positions of real satellites even if they do not run with OTFS.

For this task, we consider a User Equipment (UE) highly impacted by multipath signals, such as one placed in the city centre of Hong Kong, as described in Table I. On the transmission side, we evaluate two LEO satellites from the Starlink constellation, namely 'Starlink-1007' and 'Starlink-31658', with the properties shown in Table I and hypothetically working at f_c = 10 GHz. Specifically, these two satellites were chosen because of their difference in altitude, taking into account the strong relation between satellite altitude and ν', and because of their prototypicality within the currently existing LEO constellations. Using their TLE files, we compute the positions of each satellite during May 2024, and using the Matlab ray-tracing engine we find the Δd of the various paths over time, from which we can then compute ν'. We repeat this operation during various passes of the satellite over the UE to extract the statistical characterisation of ν'.

TABLE I: Satellite and receiver setup

UE pos. [lat, lon]	Satellite ID	Sat. alt.	Sat. vel.	Sat. passes over UE
[22.319, 114.169]	1007	∼553 km	∼27310 km/h	188
[22.319, 114.169]	31658	∼300 km	∼27900 km/h	160

B. Simulated ray-tracing results

For the two setups in Table I and considering all the multipath rays that the receiver gets with 3 or fewer reflections, the results for the characterisation of τ' and ν' are shown in Fig. 2 and Fig. 3, respectively.

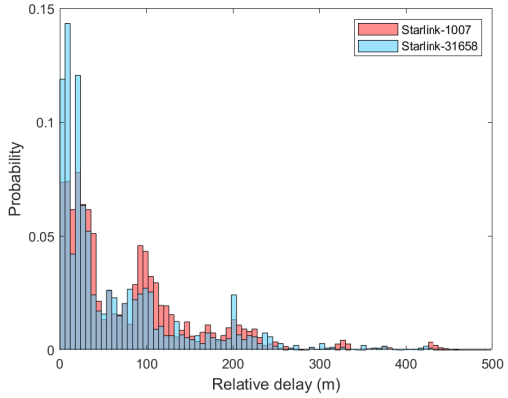

Fig. 2: Distribution of τ' for the described LEO scenarios.

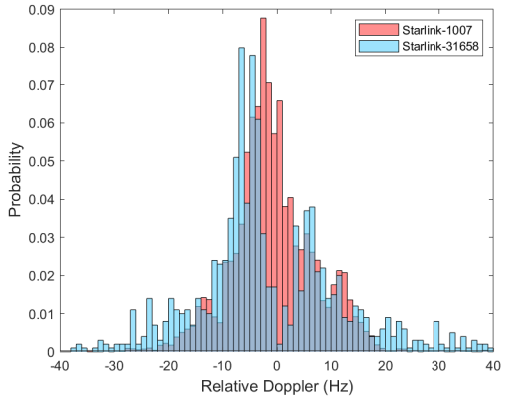

Fig. 3: Distribution of ν' for the described LEO scenarios.

From these results, the average $|\nu'|$ for Starlink-1007 is found to be 5.9 Hz, while its average $|\tau'|$ is 19.34 m. In comparison, for Starlink-31658, these values reach 10.31 Hz and 16.18 m, respectively. As expected, the faster 'Starlink-31658' produces bigger values of $|\nu'|$ while τ' remains independent.

IV. OTFS Ranging Accuracy Performance

We consider a simulation setup with B = 10 MHz and F_s = 50 MHz, and compare OTFS to BPSK, the standard modulation in GNSS, using the aforementioned Starlink satellites. Notably, these satellites do not use OTFS and are considered herein only as a hypothetical case, to showcase the potential advantages of OTFS for any constellation of LEO satellites.

Let us assume that we have a requirement on achieving a ranging error below 1 m when τ' = 30 m for 97.5% of Doppler cases when using 'Starlink-31658'. The τ' = 30 m case is considered because it is a critical case for both OTFS and BPSK for the given B [24]. Considering Eq. (5) and the Doppler distribution shown in Fig. 3, we find that a $\Delta\nu$ = 2.5 Hz fits this requirement. For the given B, an M = 667 and an N = 6000 are configured to reach the target $\Delta\nu$.

A. Simulated delay accuracy against E_s/N_0

Using the signal model in Eq. (4), the average ν' values found using 'Starlink-1007' and 'Starlink-31658', and considering the critical $\tau' = 30$ m case, the Root-Mean-Square

Error (RMSE) of the delay estimation is computed for various values of E_s/N_0, with E_s the received signal energy, and taking that the multipath's power is 3 dB below that of the LoS. Fig. 4 compares these results between OTFS and BPSK modulations, and with their respective Cramér-Rao Bounds (CRB). For the delay estimation, the considered CRB only takes into account the presence of the LoS, and is given by $\mathrm{CRB}(\tau) \approx \left(\alpha(B/2)^2 \cdot \frac{E_s}{N_0/2}\right)^{-1}$, with α depending on the Root-Mean-Square (RMS) bandwidth and approximated as $[\alpha]_{\mathrm{OTFS}} \approx \frac{4\pi^2}{3}$ and $[\alpha]_{\mathrm{BPSK}} \approx 4.41$ [26].

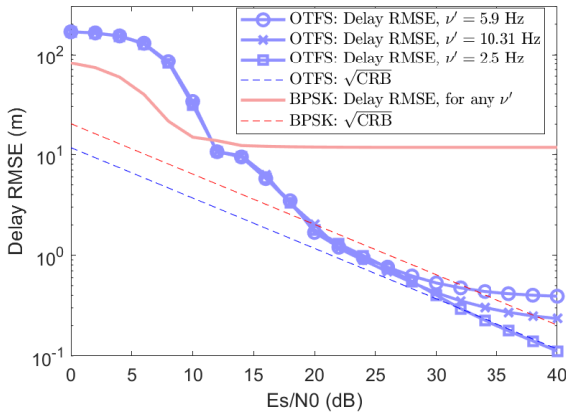

Fig. 4: Delay RMSE for representative values of ν' in the Starlink constellation, for τ' = 30 m and the set UE position.

Fig. 4 shows the improvements of OTFS with respect to BPSK. While the saturation level given by the presence of multipath is high for BPSK, OTFS keeps it low due to its fine Doppler resolution that allows for the distinction of LoS and multipath. Interestingly, Eq. (5) shows that if ν' equals $n\Delta\nu$, with $n \in \{0, 1, 2, ...\}$, then $e_{\tau,\mathrm{MP}} = 0$ m and the delay RMSE follows the CRB, such as the case of $\nu' = 2.5$ Hz. For other values of ν', the saturation levels depend on $e_{\tau,\mathrm{MP}}$. Given that the average $|\nu'|$ of 'Starlink-1007' is lower than that of 'Starlink-31658', the saturation level of the prior is higher. For BPSK, since its Doppler resolution is much worse than that of OTFS, varying ν' has negligible impact, and the LoS cannot be discerned from the multipath through Doppler refinement.

B. Statistical analysis of OTFS multipath ranging accuracy

Next, we take into consideration all the values of ν' given by both satellites in Fig. 3, and the case of $\tau' = 30$ m, and we compute the delay RMSE for each. For this experiment, we focus solely on the impact of the multipath without considering the channel noise, to evaluate its affectation on both modulations. We put each ν' value into our simulator, which considers one multipath with a power 3 dB lower than the LoS. The results in Fig. 5 display the histogram of the OTFS delay RMSE for both satellites, compared with BPSK.

As expected, the error using BPSK is high, unchanging, and equal in both satellites, but for OTFS the error differs due to the different distributions of ν' of the two considered satellites. Particularly, OTFS performs best for 'Starlink-31658', which is expected from Eq. 5 since the average $|\nu'|$ is higher, given the lower altitude of the satellite. Table II shows the statistical results of the delay RMSE for the two satellites.

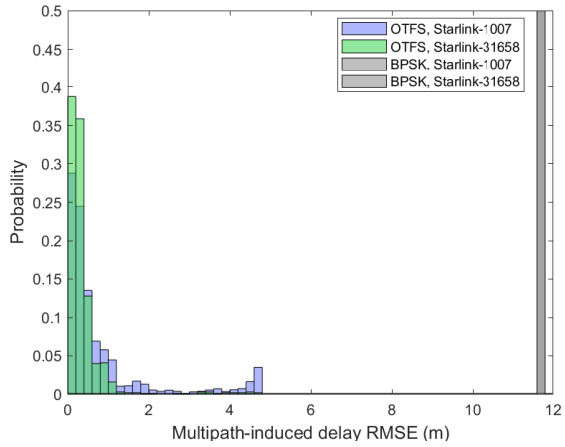

Fig. 5: Delay estimation error induced only by the presence of multipath, for τ'= 30 m and the ν' distributions in Fig. 3.

TABLE II: OTFS and BPSK performance comparison

City	Satellite ID	OTFS τ_{RMSE}	OTFS % $\leq$ 1 m	BPSK τ_{RMSE}
Hong Kong	1007	1.45 m	79.48 %	11.78 m
Hong Kong	31658	0.68 m	95.50 %	11.78 m

These results show that the requirement we set for $e_{\tau,\mathrm{MP}}$ is almost achieved, with the vast majority of the OTFS delay error for 'Starlink-31658' falling below 1 meter, and a delay RMSE of 0.68 m. The small discrepancy of these results from the requirement comes from Eq. (5) being an approximation.

These findings indicate that, if OTFS were to be used in LEO satellites, such as Starlink, prominent advantages in terms of positioning accuracy in multipath scenarios could be obtained and tailored to a specific requirement. They also show its dependency with the $\nu'/\Delta\nu$ ratio; the slower the LEO satellite, the lower the ratio and the lower the delay accuracy. Given the direct relation between them, better accuracy can be achieved by lowering $\Delta\nu$, at the cost of higher complexity.

V. Conclusions

In conclusion, the prospect of using OTFS with LEO satellites in a real urban multipath scenario has been studied and compared with the standard BPSK modulation in GNSS. OTFS shows important gains in ranging estimation accuracy in the presence of multipath for the LEO channel due to the relation between the fine Doppler resolution of the prior and the relative Doppler of the latter. We have obtained the cost function of the multipath delay error that depends on the parameters of OTFS and on the distribution of the relative delay and Doppler, from which OTFS can be configured to obtain a certain multipath ranging error. Given the dependancy with the relative delay and Doppler distributions, they have been analysed simulating satellites 'Starlink-1007' and 'Starlink-31658' flying over downtown Hong Kong, for numerous passes of these satellites. From them and from an imposed requirement on the accuracy of the ranging estimation, the OTFS parameters keeping with it have been defined. Finally, given their definition, the ranging estimation accuracy results have been obtained and compared with BPSK, showcasing the clear gains of OTFS for LEO-PNT in multipath scenarios and the compliance with said ranging accuracy requirement.

REFERENCES

[1] A. Ojala, S. Fraccastoro, and M. Gabrielsson, "Internationalization of indoor positioning platform firms: Insights from loose coupling theory," in *Proceedings of the 57th Hawaii International Conference on System Sciences*. Hawaii International Conference on System Sciences, 2024.

[2] E. D. Kaplan and C. Hegarty, *Understanding GPS/GNSS: Principles and Applications*. Artech house, 2017.

[3] H. Benzerrouk, Q. Nguyen, F. Xiaoxing, A. Amrhar, A. V. Nebylov, and R. Landry, "Alternative PNT based on Iridium Next LEO Satellites Doppler/INS Integrated Navigation System," in *Proc. Int. Conf. on Integrated Navigation Syst.*, 2019, pp. 1–10.

[4] W. Stock, R. T. Schwarz, C. A. Hofmann, and A. Knopp, "Survey On Opportunistic PNT With Signals From LEO Communication Satellites," *IEEE Commun. Surveys & Tutorials*, 2024.

[5] F. S. Prol, R. M. Ferre, Z. Saleem, P. Välisuo, C. Pinell, E. S. Lohan, M. Elsanhoury, M. Elmusrati, S. Islam, K. Çelikbilek, K. Selvan, J. Yliaho, K. Rutledge, A. Ojala, L. Ferranti, J. Praks, M. Z. H. Bhuiyan, S. Kaasalainen, and H. Kuusniemi, "Position, navigation, and timing (pnt) through low earth orbit (leo) satellites: A survey on current status, challenges, and opportunities," *IEEE Access*, vol. 10, 2022.

[6] L. Ries, M. C. Limon, F.-C. Grec, M. Anghileri, R. Prieto-Cerdeira, F. Abel, J. Miguez, J. V. Perello-Gisbert, S. D'Addio, R. Ioannidis *et al.*, "LEO-PNT for augmenting Europe's space-based PNT capabilities," in *Proc. IEEE/ION Position, Location and Navigation Symposium (PLANS)*, 2023, pp. 329–337.

[7] D. Egea-Roca, J. A. López-Salcedo, G. Seco-Granados, and E. Falletti, "Comparison of several signal designs based on chirp spread spectrum (CSS) modulation for a LEO PNT system," in *Proc. ION GNSS+*, 2021, pp. 2804–2818.

[8] M. Hosseinian, J. P. Choi, S.-H. Chang, and J. Lee, "Review of 5G NTN standards development and technical challenges for satellite integration with the 5G network," *IEEE Aerosp. Electron. Syst. Mag.*, vol. 36, no. 8, pp. 22–31, 2021.

[9] J. Garcia-Molina, S. Wallner, C. Vazquez, G. De Pasquale, J. Del Peral-Rosado, G. Da Broi, T. Schmitt, F. Melman, J. Parro, F. Soualle *et al.*, "Quasi-pilot signals: Acquisition and fast time ambiguity resolution," in *Proc. Workshop on Satellite Navigation Technology (NAVITEC)*, 2022, pp. 5–7.

[10] R. Hadani, S. Rakib, M. Tsatsanis, A. Monk, A. J. Goldsmith, A. F. Molisch, and R. Calderbank, "Orthogonal Time Frequency Space Modulation," in *2017 IEEE Wireless Commun. and Networking Conference (WCNC)*, 2017, pp. 1–6.

[11] P. H. Moose, "A technique for orthogonal frequency division multiplexing frequency offset correction," *IEEE Trans. on Commun.*, vol. 42, no. 10, pp. 2908–2914, 1994.

[12] S. K. Mohammed, "Derivation of OTFS modulation from first principles," *IEEE Trans. on Veh. Technol.*, vol. 70, no. 8, pp. 7619–7636, 2021.

[13] S. S. Das and R. Prasad, *Orthogonal Time Frequency Space Modulation: OTFS a Waveform For 6G*. River Publishers, 2022.

[14] S. K. Mohammed, R. Hadani, A. Chockalingam, and R. Calderbank, "OTFS—A Mathematical Foundation for Communication and Radar Sensing in the Delay-Doppler Domain," *IEEE BITS the Information Theory Magazine*, vol. 2, no. 2, pp. 36–55, 2022.

[15] L. Gaudio, M. Kobayashi, G. Caire, and G. Colavolpe, "On the effectiveness of OTFS for joint radar parameter estimation and communication," *IEEE Transs on Wireless Commun.*, vol. 19, no. 9, pp. 5951–5965, 2020.

[16] M. F. Keskin, H. Wymeersch, and A. Alvarado, "Radar sensing with OTFS: Embracing ISI and ICI to surpass the ambiguity barrier," in *Proc. IEEE Intl. Conf. on Commun. (ICC)*, 2021, pp. 1–6.

[17] P. Raviteja, K. T. Phan, Y. Hong, and E. Viterbo, "Orthogonal time frequency space (OTFS) modulation based radar system," in *Proc. IEEE Radar Conference (RadarConf)*, 2019, pp. 1–6.

[18] L. Xiao, S. Li, Y. Qian, D. Chen, and T. Jiang, "An overview of OTFS for Internet of Things: Concepts, benefits, and challenges," *IEEE Internet of Things Journal*, vol. 9, no. 10, pp. 7596–7618, 2021.

[19] Y. Ma, G. Ma, N. Wang, Z. Zhong, and B. Ai, "OTFS-TSMA for Massive Internet of Things in High-Speed Railway," *IEEE Trans. on Wireless Commun.*, vol. 21, no. 1, pp. 519–531, 2022.

[20] C. S. Reddy, P. Priya, D. Sen, and C. Singhal, "Spectral Efficient Modem Design With OTFS Modulation for Vehicular-IoT System," *IEEE Internet of Things Journal*, vol. 10, no. 3, pp. 2444–2458, 2023.

[21] M. Ubadah, S. K. Mohammed, R. Hadani, S. Kons, A. Chockalingam, and R. Calderbank, "Zak-OTFS for Integration of Sensing and Communication," *arXiv preprint arXiv:2404.04182*, 2024.

[22] E. Shtaiwi, A. Abdelhadi, H. Li, Z. Han, and H. V. Poor, "Orthogonal Time Frequency Space for Integrated Sensing and Communication: A Survey," *arXiv preprint arXiv:2402.09637*, 2024.

[23] M. F. Keskin, C. Marcus, O. Eriksson, A. Alvarado, J. Widmer, and H. Wymeersch, "Integrated Sensing and Communications with MIMO-OTFS: ISI/ICI Exploitation and Delay-Doppler Multiplexing," *IEEE Transactions on Wireless Communications*, 2024.

[24] G. Foreman-Campins, J. A. López-Salcedo, and E. S. Lohan, "Orthogonal Time Frequency Space Modulation (OTFS) for Positioning Using LEO Satellites," in *2024 36th Conference of Open Innovations Association (FRUCT)*. IEEE, 2024, pp. 188–194.

[25] Y. Hong, T. Thaj, and E. Viterbo, *Delay-Doppler Communications: Principles and Applications*. Academic Press, 2022.

[26] R. Martin, "Comments on "OFDM Transmission for Time-Based Range Estimation"," *IEEE Signal Process. Letters*, vol. 18, no. 2, p. 144, 2010.